Tuijin Jishu/Journal of Propulsion Technology
ISSN: 1001-4055
Vol. 46 No. 3 (2025)

Mitigating Third-Order Dispersion and Noise Reduction in High-Speed RoF using Integrated Approach

Saubhagya Kumar Moharana [1], Dr. Ravi kant [2], Amita Verma [3]

[1, 2, 3] *Electronics and Communication Engineering Department, School of Core Engineering, Shoolini University, Solan, Himachal Pradesh, India*

Abstract:- In this paper, we propose an integrated technique, which combines a dispersion-compensating fiber (DCF), a uniform fiber Bragg grating (UFBG), and an electronic equalizer based on the least mean square (LMS) algorithm to improve a 100 Gbps optical link by efficiently removing the third-order dispersion. The protocol is verified by running extensive simulations over the 140 km optical fiber, and it is found that Model outperforms previous proposals in signal integrity, with a quality factor of 41 and a bit error rate of 0. With a gain of 10.9 dB, Noise Figure (NF) of 29.0655 dB, and OSNR of 31.9004 dB, Model can reduce distortion and noise effects. It also compares the performance of various mode orders, probabilities, and alternate PRBS patterns to determine their individual influence on system performance. The LMS is used for adaptive equalization, in which different PRBS patterns are investigated, and an acceptable quality factor is 7.6 for a 2016 km optical link. This successful combination of DCF, UFBG, and an LMS-based electronic equalizer demonstrates Model's capability to move beyond the current performance limit of high-speed optical communication and drive next-generation network architecture.

Keywords*: Third-order Dispersion, Adaptive Equalizer, Q-factor, bit error rate.*

1. Introduction

In today's fast-paced landscape, modern communication systems face challenges driven by the demand for higher data-rate throughput and lower latency [1]. Advanced optical networks, such as radio-over-fiber (RoF), coherent optical transmission, and optical packet switching, are crucial for enabling ultra-reliable low-latency communication and enhanced broadband connectivity [1,2]. RoF technology facilitates the seamless transmission of radio signals over optical fibers (OF), thereby reducing loss and latency. Optical transmission enhances data capacity and reaches by utilizing an advanced modulation format, whereas advanced digital signal processing techniques contribute to noise reduction and improved signal integrity [1,2].

In recent years, advancements in optical fiber communication have substantially improved global communication networks. However, impairments such as chromatic dispersion and nonlinearity in optical devices cause signals to be transmitted over long distances and achieve a higher bandwidth, which is less reliable. Standard single-mode fiber (SMF) has a dispersion of approximately 16–20 ps/nm/km [1,2]. Additional impairments, such as slope and third-order dispersions, further complicate data retrieval at the receiver for higher-bandwidth applications. Chromatic dispersion in optical fibers introduces differential group delays at different wavelengths, leading to signal distortion and limited transmission distances.

To mitigate dispersion, several techniques have been proposed, including dispersion-compensating fibers, the use of different filters, and fiber Bragg gratings (FBG). The most popular techniques include the DCF and FBG. In DCF, a special fiber with a negative dispersion coefficient is used to counteract the positive dispersion of an optical fiber [2-10]. Many studies have explored the design features, applications, optimal range, and ideal conditions of DCF as efficient dispersion compensator [8-17]. The effect of the dispersion slope still causes

distortion in the signal. The dispersion slope of the DCF is negative, which counteracts the positive dispersion slope [2, 3-11]. With the advancement of photonic crystal fibers, DCF have been designed to mitigate both types of dispersion [1, 2].

As the length and data rate of the transmission increase, third-order dispersion comes into play. To mitigate this, the DCF cannot sufficiently improve the signal quality. To address the challenges associated with the DCF technique, FBGs have been proposed as an effective solution for dispersion compensation in fiber networks. FBGs have gained significant importance in the design, testing, and evolution of dispersion compensators, which are characterized by minimal nonlinear effects, low loss, and cost efficiency [18, 21]. Uniform FBGs (UFBG) reflect a single wavelength and are unsuitable for dispersion compensation because of their inability to handle broad-spectrum wavelengths [18,21].

Therefore, it is fundamental to modulate the grating period of the FBGs to reflect certain wavelength components of the optical pulse. Researchers have investigated various aspects of chirped FBGs (CFBGs), such as their design, optimization, grating periods and spans, and effective refractive index [4, 18-22].

To effectively mitigate the dispersion problem in OF communication, various compensation techniques have been suggested in previous studies, including DCF and FBGs [23] and others, such as optical phase conjugate (OPC) [2,3, 13], hybrid methods such as DCF with FBG [24], OPC with DCF [15], and OPC with DCF with FBG [15, 25-27]. Among these techniques, hybrid approaches, especially DCF with FBG, DCF with OPC, and DCF with FBG with OPC, have proven to be the most efficient for dispersion compensation.

Optical amplifiers and erbium-doped fiber amplifiers (EDFA) are widely used to mitigate signal loss over long distances. EDFAs optically amplify the signal without converting it back into the electrical signal domain, which helps maintain the integrity of the signal with minimal loss. These amplifiers are important for compensating for the attenuation of both the SMF and DCF [1, 2, 19, 28].

The signal quality is further improved when EDFAs are used in conjunction with electronic equalizers, such as those that use the Least Mean Square (LMS) or Minimum Mean Square Error (MMSE) algorithms [1, 2, 22]. Electronic equalizers eliminate signal noise and correct distortions. In order to determine the accuracy and responsiveness of the noise reduction and signal recovery process, the LMS algorithm, for example, adaptively modifies the filter coefficients using a step size and the number of forward and feedback tap coefficients [2, 7, 22]

The proposed work offers a novel method called Model, which integrates a DCF, UFBG, and electronic equalizer by applying the LMS technique. By means of efficient third-order dispersion over a 140 km OF length, this study maximizes a 100Gbps optical link. This study compares several bit-generating techniques employing PRBS using different approaches to evaluate their effects on general system performance.

2. System Design and Mathematical Modelling

System Configuration and Components

The proposed study introduces Model, an integrated approach that combines DCF, UFBG, and an electronic equalizer using the least mean squares (LMS) algorithm. The hybrid approach is optimized for high-speed optical transmission at a 100 Gbps optical link to mitigate third-order dispersion, which is critical for reducing signal distortion over a 140 km optical fiber length.

Fig 1 illustrates the simulation architecture, which is divided into four sections

- Transmitter configuration
- The optical channel
- Receiver components
- Adaptive equalizer

The parameters used throughout the simulation are listed in Table 1, and the characteristics of each component are listed in GOF) to reduce noise in Table 1.

A DCF is utilized to mitigate third-order dispersion, which is critical for reducing signal distortions over a 140 km optical fiber length. The objective is to achieve perfect dispersion compensation is described by (1)

$$L_{SMF} * D_{SMF} + L_{DCF} * D_{DCF} = 0 \quad (1)$$

where, L_{SMF} = length of single mode fiber, D_{SMF}= Dispersion in SMF, D_{DCF} = Dispersion in DCF and L_{DCF} = length of DCF.

Pulse broadening due to higher-order dispersive effects can be managed by mitigating the dispersion slope, as shown in (2).

$$S = \frac{dD}{d\lambda} = \left(\frac{2\pi c}{\lambda^2}\right)^2 \beta_3 + \left(\frac{4\pi c}{\lambda^3}\right)\beta_2 \quad (2)$$

where, $\beta_3 = \frac{d\beta_2}{d\omega} = \frac{d\beta}{d\omega^3}$, is third-order dispersion parameter. At zero-dispersion wavelength $\beta_2 = 0$ and S is proportional to β_3.

The total dispersion slope of the system is given by (3).

$$S_{Total} = L_{SMF} * S_{SMF} + L_{DCF} * S_{DCF} \quad (3)$$

Thus $S_{Total} = 0$, the slope of the DCF is negative. When the length of the DCF is selected to achieve complete compensation (D_Total =0), the condition for full dispersion slope compensation is satisfied.

The UFBG was fabricated by laterally exposing a photosensitive SMF core to periodic ultraviolet (UV) laser light, creating a spatial modulation of the refractive index. The rating reflects light that satisfies the Bragg condition, as shown in (4).

$$\lambda_{Bragg} = 2n\Lambda \quad (4)$$

where, n = refractive index, Λ = Grating period of FBG.

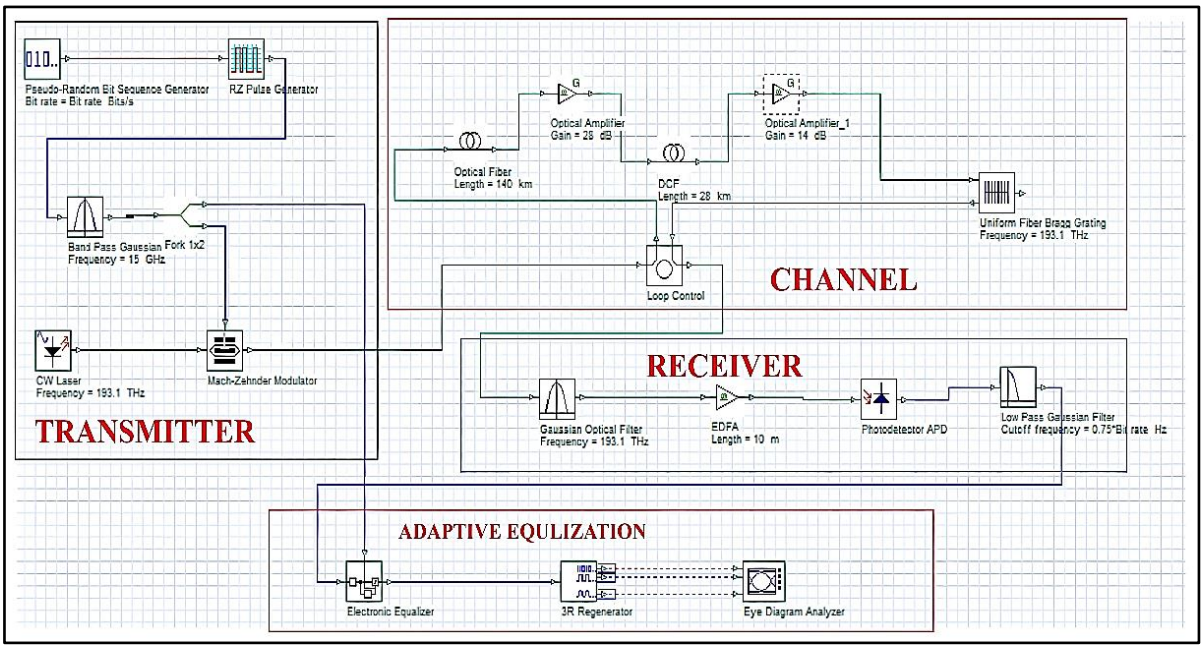

Fig. 1 Simulation Model

Light propagates through the FBG with low attenuation. The wavelengths that satisfy this condition are reflected. The main advantage of FBGs is the accurate setting and preservation of the grating wavelength.

To maintain the signal power over extended distances, optical amplifiers are employed after each span of the SMF and the DCF.

The gain of the optical amplifier is controlled by using (5)

$$G = 10\log_{10}\left(\frac{P_{out}}{P_{in}}\right) \quad (5)$$

where: P_{out} is the output power, P_{in} is the input power.

To counteract the attenuation in both SMF and DCF, using (6).

$$G = \alpha * L_F \quad (6)$$

Where: α is the attenuation per Km, L_F is the length of fiber in Km

- The required gain depends on the optical fiber length and amount of attenuation.
- Longer fiber lengths with higher attenuation require higher-gain amplifiers to maintain signal quality.

Finally, an electronic equalizer employing the LMS algorithm was used to adaptively equalize the optical signal. The LMS algorithm adjusts the tap coefficients to minimize the mean square error (MSE) between the received and transmitted signals, thereby ensuring high signal integrity and minimizing distortion over the optical link.

The electronic equalizer uses the LMS algorithm to adjust the tap coefficients of the equalizer adaptively to minimize the mean square error (MSE). The LMS update rule for the tap coefficient W_{n+1} is given in (7).

$$W_{n+1} = W_n + \mu * e_n * x_n \quad (7)$$

where: W_n is the tap coefficient of iteration n, μ is the step size of LMS algorithm, determining the rate of convergence, e_n is the error signal at iteration n, calculated as $e_n = d_n - \hat{d}_n$, Where: d_n is the desired signal and $\hat{d}_n$ is estimated signal, x_n is the input signal at iteration n.

The LMS algorithm in the electronic equalizer iteratively adjusts the tap coefficients to compensate for channel distortion and optimize the signal-to-noise ratio (SNR) of the received signal.

3. Simulation Setup Model Configuration

The present Model configuration models a single-channel optical link for fiber lengths ranging from 140 to 1680 km in length. The system was optimized for the maximum Q-factor and minimum BER by regulating the power of the optical source and combining the UFBG with an electronic equalizer.

In the transmitter section, a Continuous Wave (CW) laser with a wavelength of 1550 nm and a 10 MHz line width emits a stable carrier wave. A Mach-Zehnder external modulator (MZM) modulates the signal generated by the Pseudo-Random Bit Sequence (PRBS) in reconfigured mode pulses shaped by return zero (RZ).

In the channel,

- 140km SMF with attenuation 0.2 dB/km
- 28 km DCF with attenuation of 0.5 dB/Km, dispersion coefficient of -85 ps/nm/km, and a dispersion slope of -0.35 ps/nm^2/km

Table 1 Simulation Parameters

SIMULATION PARAMETERS	
Bit Rate	100Gbps
Sequence length	128Bits
Samples per bit	64
Number of samples	8192

To counter the loss due to attenuation, a 28 dB optical amplifier is positioned after the SMF and a 14 dB optical amplifier after the DCF using (6). Further enhancement of the dispersion compensation is achieved using a UFBG operating at a frequency of 1 THz and a wavelength of 1550 nm.

At the receiver, the signal was amplified using a 10m EDFA, and filtered by a 200 GHz optical Gaussian bandpass filter (GOF) to reduce noise.

Table 2 Model Parameters

	MODEL PARAMETERS	
Transmitter	**DEVICE NAME**	**PARAMETERS**
	PRBS	Bit rate =100Gbps
	Rz pulse generator	6.4e+012 Hz
	Cw laser	Frequency=193.1thz, Power =14 dbm
	Band pass gaussian filter	Frequency=15ghz, Bandwidth =9.6e+012Hz
Channel	SMF	Length=140km, Dispersion=17ps/nm/km Dispersion slope =0.07ps/nm^2/km
	DCF	Length=28km, Dispersion=-85ps/nm/km Dispersion slope =-0.35ps/nm^2/km, Attenuation =0.5db/Km
	Optical amplifier	Gain=28db, Noise figure=2db
	Optical amplifier1	Gain=14db, Noise figure=2db
	Ufbg	Frequency=193.1thz Bandwidth=1thz
Receiver	Gaussian optical filter	Frequency=193.1thz Bandwidth=200ghz
	EDFA	Length=10m
	Photodiode apd	Gain=3 Responsivity=1A/W
	Low pass gaussian filter	Cutoff frequency = 7.5e+010Hz
	Electronic equalizer	LMS, Step size=0.19

A high-sensitivity avalanche photodiode (APD) converts an optical signal into an electrical signal, followed by a low-pass Gaussian filter for baseband noise filtration.

Finally, the signal was subjected to electronic equalization. The LMS equalizer was configured with a

- Step size: 19
- Three forward taps
- Two feedback taps

This stage is for adaptive noise suppression and signal recovery, particularly under different PRBS modes. The continuous updating of the tap coefficient ensures optimal performance under more random sequences.

4. Result and Discussion

4.1 Signal Processing and Transmission

Initially, an alternate mode of operation of the PRBS was employed, which was then passed through an RZ pulse generator. The resulting signal was band-limited using a band-pass Gaussian filter operating at a frequency of 15

GHz. Fig. 2 shows that the band-limited electrical signal exhibits a power of 23.783 dBm at a frequency of 50GHz with a bandwidth of 3THz.

After modulation through the Mach-Zender modulator, the optical signal in Fig. 3 shows a power of 2.90 dBm at a wavelength of 1552.5 nm. The overall transmitted power was 6.293 dBm.

4.2 Dispersion Compensation

Following dispersion compensation using a combination of DCF and UFBG in the channel, the power the spectrum remains relatively stable, showing a power of 2.85 dBm at same frequency as illustrated in Fig (4).

Table 1 indicates that the SMF has a dispersion of 17 ps/nm/km for a length of 140 km. To nullify a dispersion of 980 ps/nm, a DCF of 28 km and a dispersion of -85ps/km/nm were employed.

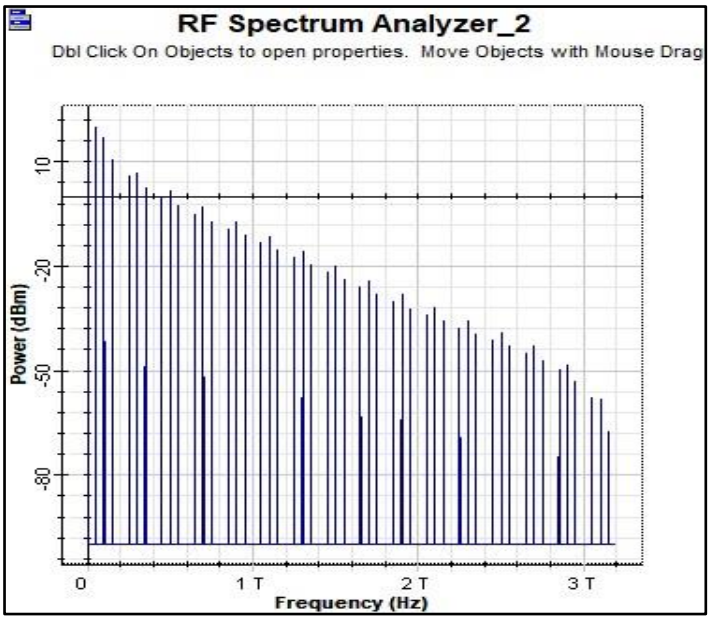

Fig. 2 Input Electrical Spectrum

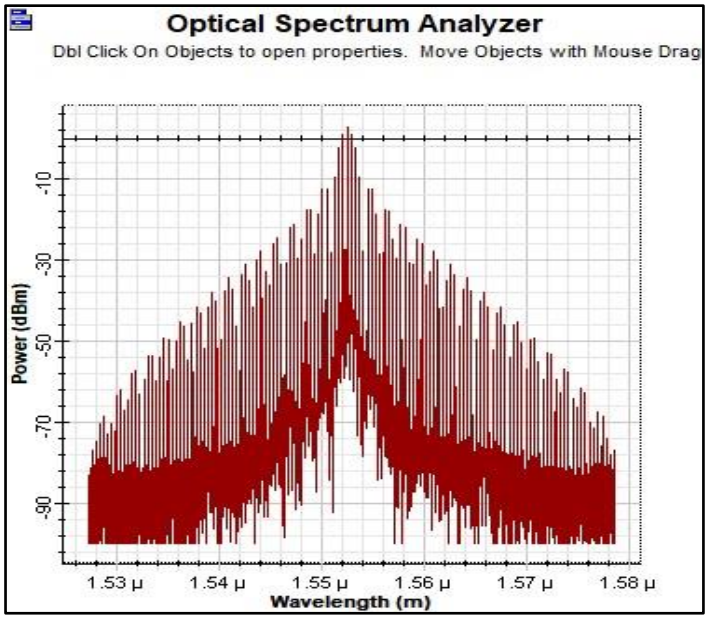

Fig. 3 Input Optical Spectrum

Using (4), the gain of the optical amplifier is set to 28 dB to counteract the attenuation of 0.2 dB/km for the optical fiber. Similarly, to compensate for the attenuation of 0.5 dB/km associated with the DCF, another optical amplifier with a gain of 14 dB was placed after the DCF.

Additionally, a negative dispersion slope of -0.35 ps/nm^2/ km in DCF successfully compensates for the accumulated dispersion slope to minimize the effect of third order dispersion, as per (6). Further compensation of the third-order dispersion is achieved using a UFBG of 1THz frequency at a wavelength of 1550 nm.

4.3 Output Optical Spectrum and Noise Analysis

After, in-line dispersion compensation by using DCF and UFBG, the output optical spectrum shows peak power of 2.85063 dBm at 1552.52 nm indicating the integrity of the transmitted signal is conserved as dBm reflects an improvement in signal efficiency of the transmitted signal is conserved as shown in Fig. 5.

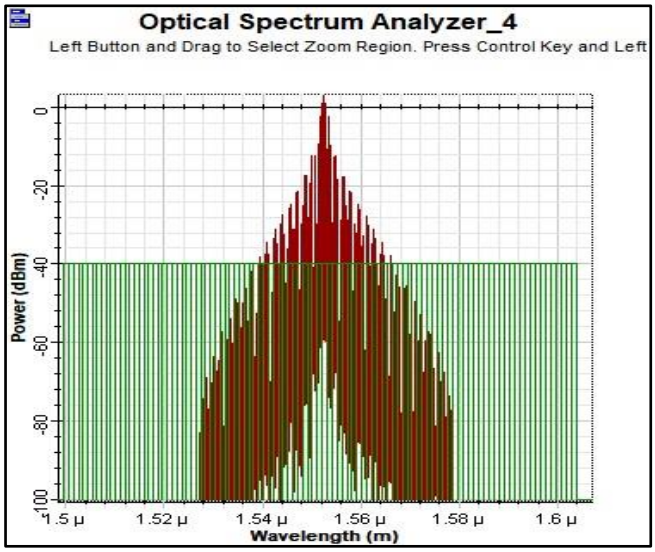

Fig. 4 Optical Spectrum After DCF

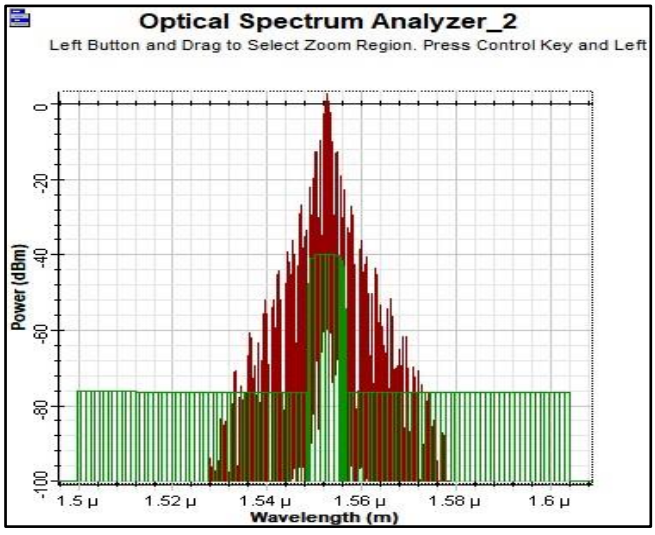

Fig. 5 Optical Spectrum After TOD compensation

The average power of 7.855 dBm reflects an improvement in signal efficiency, but with addition of noise that is being generated by the

traverse of signal for long distance plus device's additive noises. The noise power is observed to be -9.663 dBm, primarily due to amplified spontaneous noise (ASE).

4.4 Signal Recovery and Noise Suppression

At the receiver, prior to the recovery of the original electrical signal, the signal is transmitted through an optical bandpass filter with a 200 GHz bandwidth to reduce the ASE-induced noise. An EDFA of 10m was employed to enhance the strength. In Fig. 5, although the received power increases from 6.7 dBm to 17.675 dBm after filtration through the EDFA, additional noise from the ASE is also introduced. The noise power changes from -16.004 dBm to -4.465 dBm. An APD is employed to retrieve the original electrical signal, followed by a low-pass filter to suppress the low-frequency noise.

Fig. 6 (a) shows the recovered electrical spectrum, indicating a peak power of 15.462 dBm and a noise peak power of 3.219 dBm.

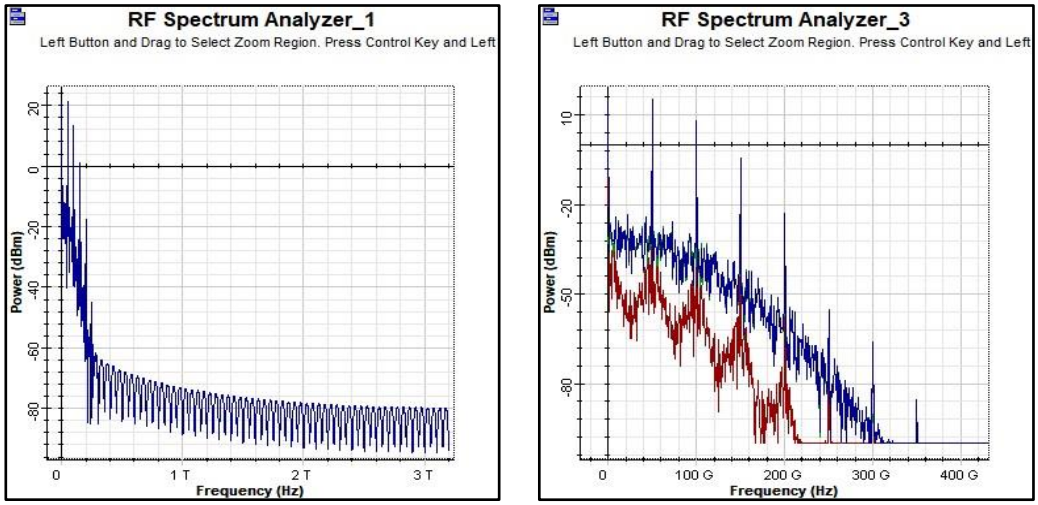

a) Before Equalization b) After Equalization

Fig. 6 Recovered Signal

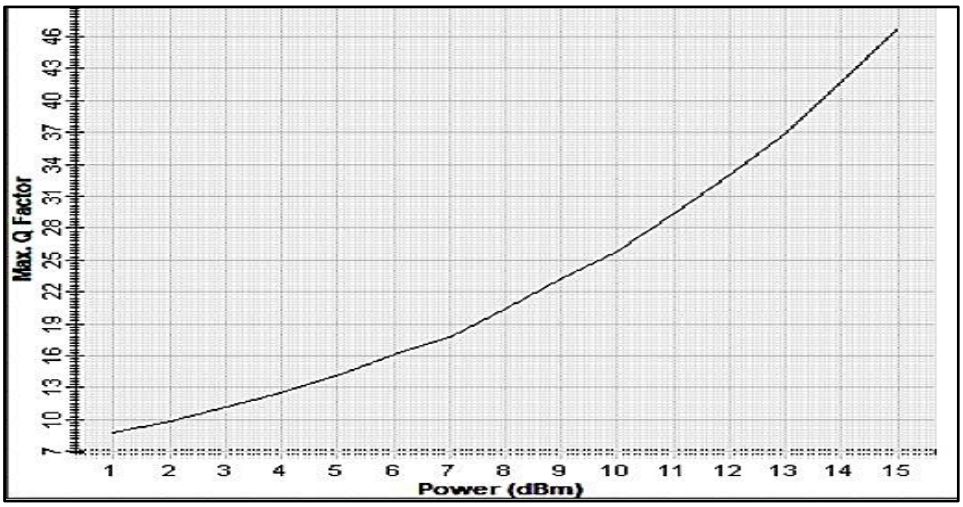

Fig. 7 Power Vs Q-factor

The average signal power and noise power were 18.636 dBm and -10.378 dBm, respectively, indicating an improvement in the model performance, albeit at the expense of the bandwidth reduction from 3 to 1THz.

4.5 Final Signal Enhancement

An electronic equalizer was used to further suppress noise and recover the original signal. The adaptive equalizer employs the LMS algorithm to recover the original signal, maintaining the signal integrity by reducing the noise

and increasing the signal bandwidth. The step size of the adaptive filter was set to 0.19, with three forward tap coefficients and two feedback tap coefficient. Fig. 6 (b), shows a highest peak power of 22.187 dBm is achieved at a frequency 50 GHz, with noise completely supressed to its minimum level of -100 dBm.

The average total power is found to be 25.375 dBm.

The signal quality and analysis of the transmission and recovery processes demonstrated substantial improvements. The initial input band-limited electrical spectrum shows a robust power of 23.783

dBm at 50 GHz with a wide 3 THz bandwidth, indicating strong signal integrity. After signal recovery and adaptive equalization, as depicted in Fig. 6 (b), the output electrical spectrum achieves a peak power of 22.187 dBm at the same frequency, with an average total power of 25.375 dBm. This reflects effective signal enhancement through noise suppression and signal recovery mechanisms, significantly reducing the noise to -100 dBm and expanding the signal bandwidth, thereby improving the overall system performance. Fig. 7 and 8 (a) show that the optimal power of 14 dBm results in the highest Q-factor of 41.14, where the BER is zero.

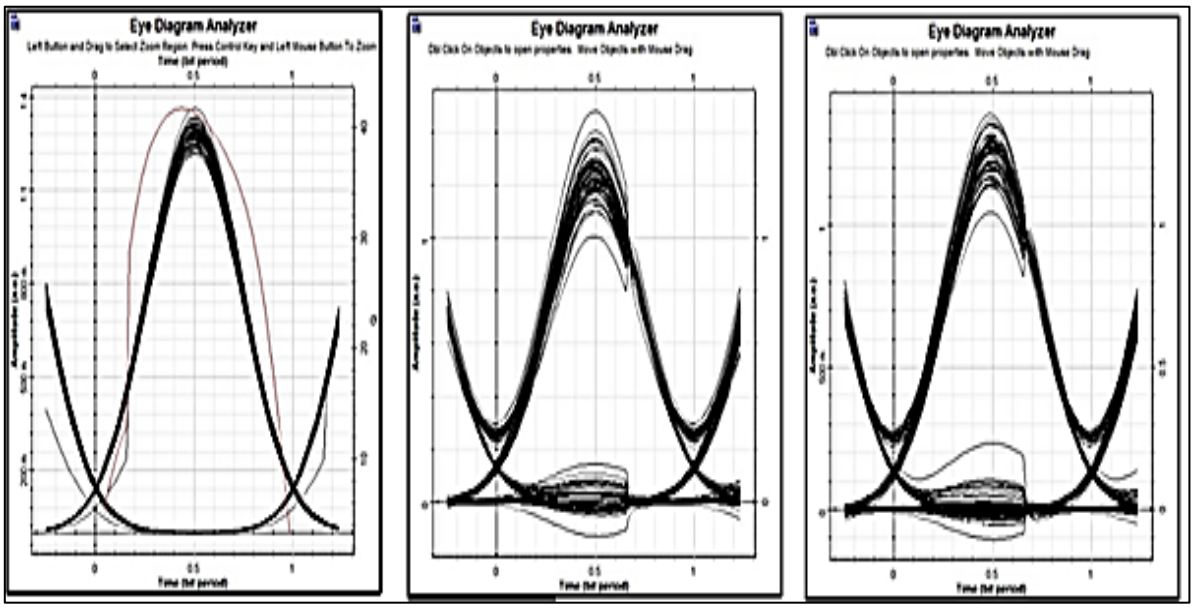

a) Alternative Mode **b) Probability mode** **c) Order Mode**

Fig. 8 Eye Diagrams

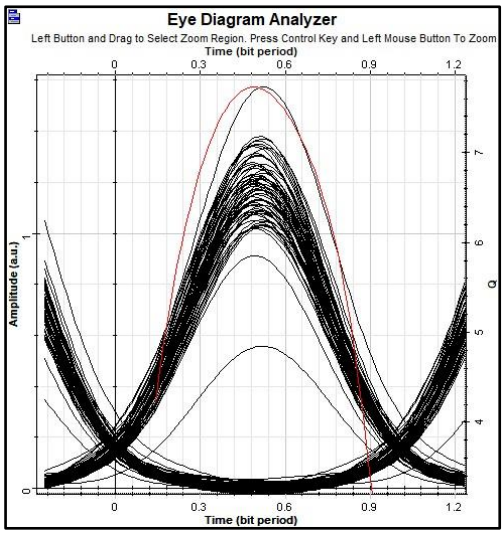

Fig. 9 Eye diagram After 12 Span

Table 3 Recorded performance metrics

Gain (dB)	Noise Figure (dB)	Input Signal (dBm)	Input OSNR (dB)	Output Signal (dBm)	Output Noise (dBm)	Output OSNR (dB)
10.904765	29.065524	3.004961	103.00496	13.909726	17.990662	31.900388

After 12 spans, the Q-factor remains at 7.6, enabling the transmission of the signal over an optical link spanning 2016 km, as illustrated in Fig. 9. The system operated at a laser power of 12 dBm with an optical, resulting in a net gain of 10.84 dB and an OSNR of 19.02 dB, as shown in Fig. 10 (a).

The optical spectrum in Fig. 10 (a) shows an average power of 17.73 dBm but carries significant noise (-22.07 dBm). In Fig 10 (b), the received signal before equalization (18.131 dBm with -1.043 dBm noise) highlights the need for noise suppression.

After equalization, as shown in Fig. 10 (c), the model effectively cancels the noise and improves the

received power to 26.646 dbm. This demonstrates the robustness and feasibility of the optical communication system in maintaining signal integrity over long distances, showcasing its potential for practical deployment in extensive optical networks.

Recorded Performance Metrics

Table 3 shows the results of the model simulation of a 140 km SMF optical system, which indicates a stable gain of 10.904 dB and an NF of 29.06 dB.

The input signal remained consistently at 3.004 dB, whereas the output signal was maintained at 13.909 dBm for optical signals. The output noise level was -17.99 dBm, resulting in an OSNR of 31.9 dB.

These metrics were consistent across frequency variations of approximately 1.55 μm. The model demonstrated the system's ability to effectively preserve signal quality and integrity, validating its suitability for long-distance optical transmission applications.

Table 4 Measured Power for various modes of PRBS

	Operation Modes of PRBS		
Parameters	**Order**	**Alternate**	**Probability**
Input Power	12 dBm	14 dBm	12 dBm
Power At Channel	6.675 dBm	6.675 dBm	6.675 dBm
Power After Channel	7.75 dBm	8.26 dBm	7.015 dBm
Received Power	25.217 dBm	17.95 dBm	25.85 dBm

Table 5 Comparison of Q-factor and BER for various modes of PRBS

Operation Modes of PRBS	**Step Size**	**Q-Factor**	**BER**
Order	0.2	39	0
Alternate	0.19	41	0
Probability	0.2	30.129	9.99E-200

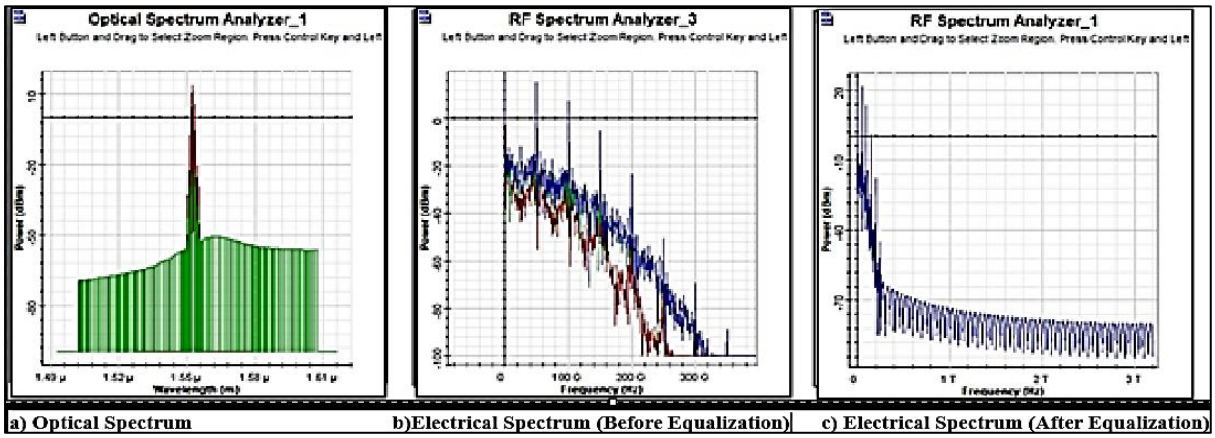

Fig. 10 Spectrums after 2016 km optical distance

Comparisons Between Operating Modes on System Performance

Tables 4 and 5 underscore that the PRBS operation at 14 dBm input power exhibits the highest Q-factor of 41 and zero BER, indicating optimal signal quality. At 12 dBm input power, the Q-factor remains high at 39 with a negligible BER, demonstrating a robust performance, as shown in Fig. 8(a).

However, the probability-based operation at the same input power shows a lower Q-factor of 30.129 and a non-zero BER of 9.99E-200, highlighting reduced signal integrity, as shown in Fig. 8 (b). These findings underscore the sensitivity of the PRBS operation to the input power levels, with higher power yielding superior signal quality and reliability.

Table 6 compares the existing models with the proposed model. In summary, the optical link experienced a loss of approximately 6.71% in peak power, and the spectral efficiency was approximately 0.0333 bps/Hz, reflecting the effectiveness of Model integration in optimizing data transmission.

Table 6 Comparison with Existing simulation results

Related Model	Bit rate	Link length	Technique Used	Max. Q-Factor	Min. BER	Input Power	Received Power
[3]	10 Gbps	180 km	Chirped FBG	12.7412	1.63E-37	10dBm	13.45dBm
[4]	100 Gbps	840 km	DCF (all Config.)	Below 7	-	Nearly 10 dBm	-
[7]	100 Gbps	120 km	UFBG with EDC (D = 0.01 ps/nm/km)	37.12	4.84E-302	10dBM	26.434
[13]	40 Gbps	220 km	DCF and Chirped FBG	7.13	4.86E-13	10 dBm	-
[14]	40	343	OTDM	11.6	1.39E-31	2 dBm	-
[26]	10 Gbps	332 km	DCF with FBG	8.5	8.52E-18		-
[28]	40	200	DCB	3.4541	0.000171	10 dBm	-
Proposed Work	**100 Gbps**	**2016 km**	**Combination of DCF, UFBG and EDC**	**7.63**	**9.62E-15**	**12 dBm**	**27.463 dBm**

5. Conclusion

This study presented using the LMS algorithm to integrate DCF, UFBG, and an electronic equalizer to reduce third-order dispersion in 100 Gbps optical links. This system remarkably improved the signal integrity by means of large simulations spanning a total distance of 2016 km of optical fiber. With a 10.9 dB gain, this system effectively reduced the third-order dispersion, thereby lowering the noise interference. This is observed from a bit

error rate of 0 for a single span of 168 km and an improved Q-factor of 41.14. Important indicators of signal quality in high-speed optical links, it also showed an modes of PRBS optical signal to noise ratio (OSNR) of 31.9004 dB and a noise figure of 29.065 dB.

Combining DCF, UFBG, and an LMS-based electronic equalizer to effectively compensate for dispersion, reduce noise, and improve signal recovery makes the model ideal for long-distance optical communication. The results enhance their dependability and efficiency since they provide a basis for practical use in real optical communication systems. Finally, current study marks a major breakthrough in high-speed optical communication, enabling next- generation network designs and supporting the construction of strong and reliable telecommunication systems.

Conflict of Interest

There is no conflict of interest among the authors.

Fundings

Not applicable.

References

[1] G. P. Agrawal, Fiber-Optic Communication Systems. 2010.
[2] H. Hamam and S. Guizani, Optical Fiber Communications, vol. 1. 2011. doi: 10.1002/9781118256053.ch44.
[3] M. L. Meena and R. Kumar Gupta, “Design and comparative performance evaluation of chirped FBG dispersion compensation with DCF technique for DWDM optical transmission systems,” Optik (Stuttg)., vol. 188, pp. 212–224, 2019, doi: 10.1016/j.ijleo.2019.05.056.
[4] F. Paloi, T. Mirza, and S. Haxha, “Optimisation of dispersion compensating in a long-haul fibre for RF transmission of up to 100 Gbit/s by using RZ and NRZ formats,” Optik (Stuttg)., vol. 131, pp. 640–654, 2017, doi: 10.1016/j.ijleo.2016.11.202.
[5] V. Dilendorfs, M. Parfjonovs, A. Alsevska, S. Spolitis, and V. Bobrovs, “Influence of dispersion slope compensation on 40 Gbit/s WDM-PON transmission system performance with G.652 and G.655 optical fibers,” Prog. Electromagn. Res. Symp., vol. 2017-Novem, no. Cd, pp. 598–604, 2017, doi: 10.1109/PIERS-FALL.2017.8293207.
[6] R. Gupta and M. L. Meena, “Design and Analysis of Hybrid Dispersion Compensation Techniques for 32×40Gbps DWDM Optical Transmission Systems,” pp. 0–32, 2022, [Online]. Available: https://doi.org/10.21203/rs.3.rs-1653304/v1
[7] A. Sharma, S. Sharma, A. Sharma, I. Singh, and S. Bhattacharya, “Simulation and analysis of dispersion compensation using proposed hybrid model at 100gbps over 120km using SMF,” Int. J. Mech. Eng. Technol., vol. 8, no. 12, pp. 600–607, 2017.
[8] M. , Kaur, H. Sarangal, and P. Bagga, “Dispersion Compensation with Dispersion Compensating Fibers (DCF),” Ijarcce, vol. 4, no. 2, pp. 354–356, 2015, doi: 10.17148/ijarcce.2015.4280.
[9] Rekha and M. K. Rai, “Analysis and comparison of dispersion compensation by DCF schemes and fiber bragg grating,” Int. J. Control Theory Appl., vol. 9, no. 41, pp. 165–176, 2016.
[10] G. M. Ranjeet Kaur1, “Comparative Study of Dispersion Compensating Techniques Pre, Post and Mix with 8 Channels,” Int. J. Adv. Res. Electr. Electron. Instrum. Eng., vol. 6, no. 7, pp. 5876–5887, 2017, doi: 10.15662/IJAREEIE.2017.0607047.
[11] R. Darwis, O. N. Samijayani, A. Syahriar, and I. Arifianto, “Performance analysis of dispersion compensation fiber on NRZ and RZ modulation with difference power transmission,” Univers. J. Electr. Electron. Eng., vol. 6, no. 3, pp. 159–166, 2019, doi: 10.13189/ujeee.2019.060310.
[12] F. Khair, F. Fahmi, D. Zulherman, I. Teknologi Telkom Purwokerto, J. DI Panjaitan No, and J. Tengah, “Performance Comparison of Dispersion Compensation Schemes Using DCF in DWDM Optical Network,” J. Infotel, vol. 10, no. 02, pp. 62–67, 2018, doi: 10.20895/infotel.v10i2.362.

[13] A. Kumar, I. Singh, S. Bhattacharya, S. Sharma, R. P. Dwivedi, and H. I. Lee, "Comparison of Different Dispersion Compensation Techniques at 100Gbps Over 120Km Using Single Mode Fiber," Int. J. Innov. Technol. Explor. Eng., no. 8, pp. 2278–3075, 2019.
[14] N. Nerkar, M. Kadu, and R. Labade, "A Novel Architecture to Reduce Dispersion in Fiber by Using Pre, Post and Symmetrical DCF Methods," vol. 137, pp. 610–616, 2017, doi: 10.2991/iccasp-16.2017.87.
[15] A. Asiwal and D. Dhawan, "Comparative Analysis of Dispersion Compensating Fiber (DCF) and Optical Phase Conjugation (OPC) used for Dispersion Compensation," Ijireeice, vol. 5, no. 7, pp. 14–19, 2017, doi: 10.17148/ijireeice.2017.5703.
[16] S. na and M. Kaur, "Performance Comparison of Pre-, Post-, and Symmetrical Dispersion Compensation using DCF for 64 x 40 Gb/s DWDM System," Int. J. Electron. Commun. Eng., vol. 4, no. 7, pp. 1–6, 2017, doi: 10.14445/23488549/ijece-v4i7p101.
[17] M. Y. Hamza and I. Hayee, "Performance improvement of 40 Gb/s WDM systems by optimization of dispersion map," Appl. Inf. Commun. Technol. AICT 2016 - Conf. Proc., 2017, doi: 10.1109/ICAICT.2016.7991755.
[18] M. Singh and R. B., "Analysis of Dispersion Compensation using Fiber Bragg Grating in Optical Fiber Communication System," Int. J. Comput. Appl., vol. 126, no. 5, pp. 1–5, 2015, doi: 10.5120/ijca2015906046.
[19] S. Vishwakarma, A. Ghosh, and E. Student, "A Simulation Approach in Optical System for Dispersion Compensation Using a FBG," pp. 115–123, 2018.
[20] P. Berwal, "Optical System Design Using Fiber Bragg Grating with RZ Modulation Format," vol. 2, no. 7, pp. 111–113, 2014.
[21] I. Nsengiyumva, E. Mwangi, and G. Kamucha, "A comparative study of chromatic dispersion compensation in 10 Gbps SMF and 40 Gbps OTDM systems using a cascaded Gaussian linear apodized chirped fibre Bragg grating design," Heliyon, vol. 8, no. 4, p. e09308, 2022, doi: 10.1016/j.heliyon.2022.e09308.
[22] B. Prasad, B. Mallick, K. C. Patra, and N. K. Barpanda, "Dsp based chromatic dispersion equalization techniques in PDM-QPSK receivers," Proc. Int. Conf. Trends Electron. Informatics, ICOEI 2019, vol. 2019-April, no. Icoei, pp. 302–307, 2019, doi: 10.1109/icoei.2019.8862630.
[23] A. Sharma, S. Singh, and B. Sharma, "Investigations on Dispersion Compensation using Fiber Braggs Grating," Int. J. Comput. Appl., vol. 73, no. 2, pp. 34–43, 2013, doi: 10.5120/12715-9529.
[24] A. Bhardwaj and G. Soni, "Performance Analysis of 20Gbps Optical Transmission System Using Fiber Bragg Grating," Int. J. Sci. Res. Publ., vol. 5, no. 1, pp. 8–11, 2015, [Online]. Available: www.ijsrp.org
[25] H. Mahmood, "DCF with FBG for Dispersion Compensation in Optical Fiber Link at Various Bit Rates using Duobinary Modulation Format," Eng. Technol. J., vol. 36, no. 5A, pp. 514–519, 2018, doi: 10.30684/etj.36.5a.6.
[26] T. F. Hussein, M. R. M. Rizk, and M. H. Aly, "A hybrid DCF/FBG scheme for dispersion compensation over a 300 km SMF," Opt. Quantum Electron., vol. 51, no. 4, pp. 1–16, 2019, doi: 10.1007/s11082-019-1823-y.
[27] A. Singh and A. Sureel, "Study of POST and PRE-Scheme of Dispersion Compensation in a 32 Channel DWDM Network with NRZ , RZ and Encoded Transmitter," vol. 9, no. 2, pp. 86–89, 2021.
[28] T. Xie, M. Asif, H. Ali, and H. M. R. Afzal, "Reparation of chromatic dispersion using dispersion compensation bank and bit-error rate analysis at various power levels in 40 Gbps fiber optics system," Proc. - 2014 7th Int. Congr. Image Signal Process. CISP 2014, pp. 1058–1062, 2014, doi: 10.1109/CISP.2014.7003936.